CHEMICAL AND STOCHASTIC MODELING OF LIGNIN HYDRODEOXYGENATION

Peter M. Train and Michael T. Klein

Center for Catalytic Science and Technology
and
Department of Chemical Engineering
University of Delaware
Newark, DE 19716

Abstract

An *a priori* Monte Carlo simulation of the product spectrum resulting from the thermal and catalytic depolymerization of lignin has been developed. The simulation combines model compound reaction pathways and kinetics, deactivation parameters, and stochastic models of polymer diffusion into a Markov-chain based simulation of the reaction of lignin polymers. Predicted product class ratios of single-ring phenolics were in reasonable agreement with experimental data pertaining to lignin liquefaction, especially as regards neat pyrolysis. The advantage of catalytic liquefaction was suggested by the increase in single-ring product yields, especially those of phenols and hydrocarbons, relative to pyrolysis.

Introduction

The intensity of research in the U. S. and abroad into the liquefaction of coal has largely been directed toward reduction of the demands on petroleum feedstocks. Both traditional fossil fuel feedstocks and alternative feeds are rich in sulfur and nitrogen, and removal of these heteroatoms has therefore been studied in detail. Oxygen removal is less well studied although large quantities of oxygen are found in biomass and coals. Herein we focus attention on the former feed.

Wood comprises cellulose, hemicellulose and lignin portions, with proportions of the latter typically one-third by weight. The potential for upgrading lignin to useful chemicals or fuel additives has been demonstrated [5]. Moreover, the structural elements of lignin are well enough understood to make it an attractive substrate for study. The study of lignin thus provides an opportunity for generalization about the reactions of lignites and low-rank coals that share similar structural features.

Lignin pyrolysis is to rather low yields of useful single-ring phenolics (10-15%), and as many as 33 different phenolics form, each in low yield, rather than any one in a usefully high yield [1,3,7,8,9,10]. Much of the original lignin weight is lost to a high molecular weight char, suggested by model compound experiments to form via a polymerization of ortho oxygen-containing guaiacyl moieties characteristic of lignin [11]. Petrocelli [16] has suggested that the catalytic hydrodeoxygenation (HDO) of lignin should reduce char formation by removing some of the guaiacyl oxygen as water and thus circumventing the polymerization to char; the single-ring phenolic fraction is also substantially simplified as a result.

This motivated the development of a model compound based and thus predictive computer simulation of lignin liquefaction. This would allow scrutiny of the feasibility of various lignin upgrading schemes by testing various processing strategies in a quantitative link of the competing factors of reaction, diffusion, catalyst deactivation, substituent effects and multiple bond identities.

A stochastic model of depolymerization has several advantages over deterministic models. First, substrate heterogeneities, including substituent effects, multiple linkage types, and an unusual molecular weight distribution are easily addressed in a stochastic model. Second, a Monte Carlo model can account for the molecular weight of each reactive moiety separately, which facilitates proper modeling of the diffusion and reaction in a porous catalyst. Thus, the classic approximation of equal reactivity need not be invoked. Finally, the processes involved in chemical kinetics may well be stochastic, so it seems reasonable to model them as such.

Background and Model Development

Stochastic Kinetics

The stochastic approach to chemical kinetics is well known [14] and has been applied by McDermott [13] and Squire [19] to model the decomposition of a simplified lignin polymer and coal, respectively. In one approach, the stochastic simulation of the polymer decomposition begins by dividing the total reaction time into small time steps of equal duration, after the passage of which the reactions of the polymer bonds are tested by comparing a characteristic reaction probability to a random number. Reaction occurs when this transition probability is greater than the drawn random number. In this manner, each bond along the polymer chain is tested for reaction, and the procedure is repeated through time in increments of Δt until the desired final time is reached. This process is equivalent to mapping out a first-order Markov chain through time, as illustrated in Figure 1, where the new physical state of the system depends solely on the previous state of the polymer. The Monte Carlo simulation is the average result of a large number of Markov chains.

The transition probability for the first-order reaction of A to B follows the Poisson distribution and has the general form shown in Equation 1:

$$P_{AB} = 1 - e^{-k_{AB}\Delta t} \tag{1}$$

Thus both the size of the time step and the overall rate constant dictate the likelihood of reaction. For the present model of the catalytic liquefaction of lignin, the appropriate k_{AB} for a given moiety included factors for diffusion limitations and catalyst age. Thus, the transition probability for each reactive moiety in lignin had a catalytic and thermal component, as in Equation 2:

$$P = 1 - e^{-(\eta\Phi w_c k_c + k_t)\Delta t} \tag{2}$$

where η = catalytic effectiveness factor; Φ = catalyst activity; k_c = intrinsic catalytic reaction rate constant, $l/g_c{\cdot}s$; w_c = catalyst bed loading, g_c/l; Δt = reaction time step, s; k_t = intrinsic thermal reaction rate constant, s^{-1}.

Lignin Structure

The lignin reactant was assembled randomly. This was accomplished by transferring the detailed information contained in chemical models for lignin structure [4,18] into probabilities of substituent and bond types present on each position of an average aromatic ring as illustrated in Figure 2. Four ring positions were required to define a lignin ring, and two of these identified as P1 and P2 contained primarily oxygen-bearing substituents and linkages, whereas the other two identified as H1 and H2 contained hydrocarbon substituents. Coupling this substituent distribution information with the details of the initial distribution of lignin molecular weights allowed random generation of linear lignin polymers of appropriate lengths.

In practice, a drawn random number was placed onto the integral probability distribution of substituent and linkage types at each of the four ring positions. This assembly determined each substituent and linkage type along a lignin polymer chain whose length was determined by placing a drawn random number on the integral molecular weight probability distribution. Repetition according to the Monte Carlo technique allowed generation of an appropriate starting lignin.

Lignin Reactions

The reaction pathways and intrinsic kinetics parameters were deduced from related model compound experiments reported elsewhere [6,8,11,12,13,15,16,20]. The operative reaction pathways and kinetics parameters elucidated are summarized in Table 1.

Catalyst Deactivation

Model compound reactions in a flow microreactor allowed observation of the decay of catalyst activity with time on stream. This is illustrated in Figure 3 for the reaction of 2-hydroxydiphenylmethane at 2250 psig H_2, 250°C and WHSV=0.49 hr^{-1} [20]. Best fit models relating the observed activity losses to the quantity of oxygen-containing species lost (C_c) to char were of the form

$$\Phi = e^{-\alpha C_c} \tag{3}$$

and

$$\Phi = \frac{1}{1 + \alpha C_c} \tag{4}$$

and associated deactivation parameters (α) are listed in Table 1.

Catalyst Effectiveness

The parallel events of diffusion and reaction of lignin oligomers in catalyst pores were modeled in terms of a catalyst effectiveness factor, which was a function of oligomer molecular weight and degree of polymerization (DP) as follows:

$$\eta = \frac{1}{\phi} \frac{3\phi \coth 3\phi - 1}{3\phi} \tag{5}$$

$$\phi = f(k_c, DP) \tag{6}$$

For relatively short lignin polymers (DP < 200), Rouse's model for coiling polymers in dilute solutions [17] dictated that the Thiele modulus ϕ be proportional to the square-root of DP. The diffusion of longer polymer chains (DP > 200) was modeled using de Gennes reptation theory, in which diffusion is inversely proportional to the square of molecular weight [2]. Under these conditions, and the Thiele modulus was proportional to DP.

Integration

Equations 3, 4 and 5 and the intrinsic model compound kinetics of Table 1 were integrated into a stochastic model of lignin depolymerization in terms of the transition probabilities of Equation 2. The resulting simulation was capable of predicting the product spectrum resulting from the thermal or catalytic depolymerization of kraft and milled-wood lignin.

Results and Discussion

Simulations of kraft lignin pyrolysis and catalytic liquefaction were at 380 and 400°C. The predicted product yields from catalytic liquefaction of kraft lignin at 380°C, 2250 psig and 2.47 g_{lignin}/g_c in a batch reactor (case 1) illustrated in Figure 4 increase with time to 0.23 and 0.17 for single-ring products and char, respectively after 30 min.

Figure 4 also illustrates the effects of catalyst deactivation and internal transport. Simulations run in which both were either included or neglected provided limiting cases. Intrinsic kinetics resulted in the highest yields of single-ring products and the lowest yield of char, whereas allowing for catalyst deactivation and diffusional limitations resulted in the lowest single-ring product yield and highest char yield.

The effects of polymer diffusion and catalyst deactivation were also considered separately. The remaining curves of Figure 4 illustrate. The diffusional limitation was largest initially, where polymer molecular weight was high, as both single-ring products and char evolved at lower rates initially than in the limiting case of no internal transport limitations. Moreover, inspection of the yields of these products after 30 min shows that transport had little effect on the ultimate evolution of single-ring products and char. Finally, the remaining curve in Figure 4 illustrates that the effect of catalyst deactivation was largest at longer reaction times, and lower ultimate yields of single-ring products were accompanied by greater quantities of char.

The more rapid catalytic liquefaction relative to thermal depolymerization is illustrated in Figure 5 as a plot of the number molecular weight distribution parametric in reaction time. For catalytic depolymerization, a 15% yield of single-ring products was realized after only 10 min at which time the thermal yield of single- ring products was only 4%.

The temporal variation of monomer and char yield for pyrolysis and catalysis are illustrated in Figure 6 along with a measure of the selectivity to char over single-ring products. The yields of single-ring products were greatly increased upon reaction over a catalyst compared to thermal treatment alone, and char formation was decreased by roughly half. This agrees with the experimental findings of Petrocelli [16] and Train [20] that single-ring product yields were roughly doubled compared with pyrolysis. Moreover, the selectivity to char decreased rapidly to roughly 0.5 with catalytic treatment compared with the steady increase predicted with pyrolysis.

The identities of the major products in the single-ring product fraction are shown in Figure 7 as a plot of product yield versus reaction time. Whereas products containing two oxygen substituents (guaiacols and catechols) accounted for nearly half of the monomeric products evolved from pyrolysis, yields of these products were only 5% of the single-ring products formed by catalytic liquefaction. As a result, yields of both phenols and hydrocarbons increased substantially with catalytic treatment.

Finally, the simulation predictions are compared with experimental kraft lignin pyrolysis [8,9] and catalytic liquefaction [20] results in terms of the products of the monomer fraction in Figure 8. The agreement between simulated and experimental kraft lignin pyrolysis at 400°C is quite favorable. The agreement between simulated and experimental catalytic liquefaction at 380°C is still qualitatively good but quantitatively poorer.

Conclusions

The Monte Carlo simulation is a convenient and flexible tool for predicting the depolymerization of macromolecular substrates. Not only intrinsic kinetics but also catalyst deactivation and diffusional limitations can be addressed. The simulation predictions herein were in good qualitative agreement with experimental results, and agreement between predicted and experimental proportions of hydrocarbons, phenols, guaiacols and catechols in the monomer fraction was excellent. The practical significance is the prediction that removal of at least one of the oxygen-containing substituents from phenolic rings by catalytic HDO should reduce char formation and simplify the resulting phenolic product spectrum.

References

[1] Chan, R. W.-C.; Krieger, B. B. *Journal of Applied Polymer Science* 26, 1981.
[2] de Gennes, P. G. *Journal of Chemical Physics* 55(2), 1971.
[3] Domburg, G. E.; Sergeeva, V. N.; Kalninsh, A. I. *Thermal Analysis - Proceedings Third ICTA, Davos* 3, 1971.
[4] Freudenberg, K.; Neish, A. C. Springer-Verlag, New York, 1968.
[5] Goheen, D. W. *Adv. Chem. Ser.* 59, 1966.
[6] Hurff S. J.; Klein, M. T. *Ind. Eng. Chem. Fundamentals* 22, 1983.
[7] Iatridis, B.; Gavalas, G. R. *Ind. Eng. Chem. Prod. Res. Dev.* 18(2), 1979.
[8] Jegers, H. E. Master's thesis, University of Delaware, 1982.
[9] Jegers, H. E.; Klein, M. T. *Ind. Eng. Chem. Process Des. Dev.* 24, 1985.
[10] Kirshbaum, I. Z.; Domburg, G. E.; Sergeeva, V. N. *Khim. Drev.* (4), 1976.
[11] Klein, M. T. PhD thesis, Massachusetts Institute of Technology, 1981.
[12] Klein, M. T.; Virk, P. S. *Ind. Eng. Chem. Fundamentals* 22, 1983.
[13] McDermott, J. B. PhD thesis, University of Delaware, 1986.
[14] McQuarrie, D. A. Methuen & Co. LTD, London, 1967.
[15] Petrocelli, F. P.; Klein, M. T. *Macromolecules* 17, 1984.
[16] Petrocelli, F. P. PhD thesis, University of Delaware, 1985.
[17] Rouse, P. E. *Journal of Chemical Physics* 21(7), 1953.
[18] Sarkanen, K. V.; Ludwig, C. H. (editors). Wiley, New York, 1971.
[19] Squire, K. R.; Solomon, P. R.; Di Taranto, M. B.; Carangelo, R. M. *ACS Division of Fuel Chemistry Preprints* 30(1), 1985.
[20] Train, P. M. PhD thesis, University of Delaware, 1986.

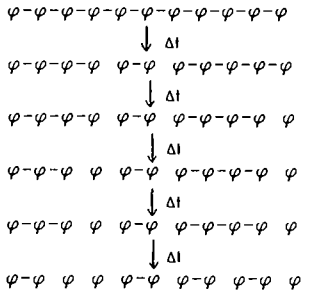

Figure 1: Random reaction trajectory of a polymer chain.

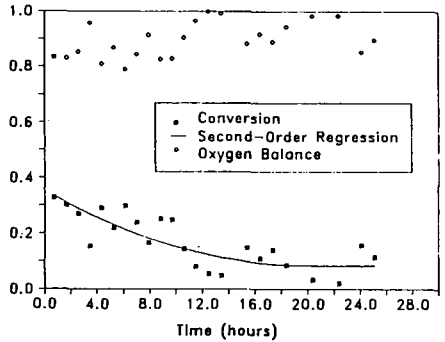

Figure 3: Catalyst deactivation in the reaction of 2-hydroxydiphenylmethane over Co-Mo/γ-Al_2O_3 at 250° C, 2250 psig, WHSV=0.49 hr^{-1}

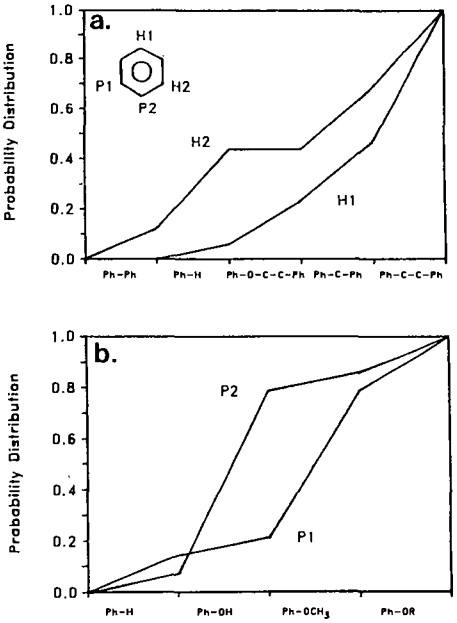

Figure 2: Cumulative probability distributions function for substituents on aromatic ring positions (a) H1, H2 and (b) P1, P2.

Reactant	Primary Products	Thermal Parameters $\log_{10}A$ (s^{-1})	E_a (kcal/mol)	Source	Catalytic Parameters $\log_{10}A$ (l/gc·s)	E_a (kcal/mol)	Source
Veratrole	Guaiacol	11.4	48	[11]	4.8	21.7	[20]
	Anisole	10.6	47.4	[11]	"	"	
	Phenol	8.7	41.8	[11]	"	"	
Guaiacol	Catechol	12.8	49.3	[11]	5.2	25.1	[16]
	Phenol	11.7	48.2	[11]	6.1	28.3	[16]
	Char	8.4	42.7	[11]	1.8	15.8	[16]
Catechol	Phenol	"	"		6.8	28.3	[16]
	Char	4.9	25.2	[8]	−0.5	10.6	[16]
Anisole	Phenol	9.1	42.2	[11]	9.8	29.7	[5]
	Benzene	12.2	69.7	[11]	"	"	
Phenol	Benzene				−1.9	6.7	[16]
Diphenylmethane	Toluene+Benzene	12.7	66.8	[16]	2.9	21.18	[20]
OHD	Phenol+Toluene	9.6	43.4	[11]	9.2	36.1	[16]
	o-Cresol+Benzene	"	"		7.8	35.2	[16]
Diphenylethane	2 Toluene	18.2	65.3	[16]			
	Ethylbenzene+Benzene	8.8	44.5	[16]			
2-Phenylphenol	Phenol+Benzene	"	"		−2	8.2	[16]
o,o'-Biphenol	2 Phenol	"	"			$-\log_{10}k_{330}=7.26$	[16]
PPE	Phenol+Ethylbenzene	11.1	65.0	[12]			
GGE	Guaiacol+AV	5	20.8	[13]			
Phenyl Ether	Phenol+Benzene	14.8	72.1	[11]	8.7	35.4	[16]
4-Phenoxyphenol	2 Phenol				8.7	32.2	[20]

OHD = 2-hydroxydiphenylmethane
PPE = Phenethyl Phenyl Ether
GGE = Guaiacylglycol-β-guaiacyl Ether
AV = Acetovanillone

Deactivation Parameters [20]	α (mol O/gc)	Form of Activity Function
Single-Ring Phenolics	589.2	Equation 4
Carbon Linkages	273.5	Equation 3
Ether Linkages	28.8	Equation 3

Table 1: Summary of model compound kinetics and reaction pathways.

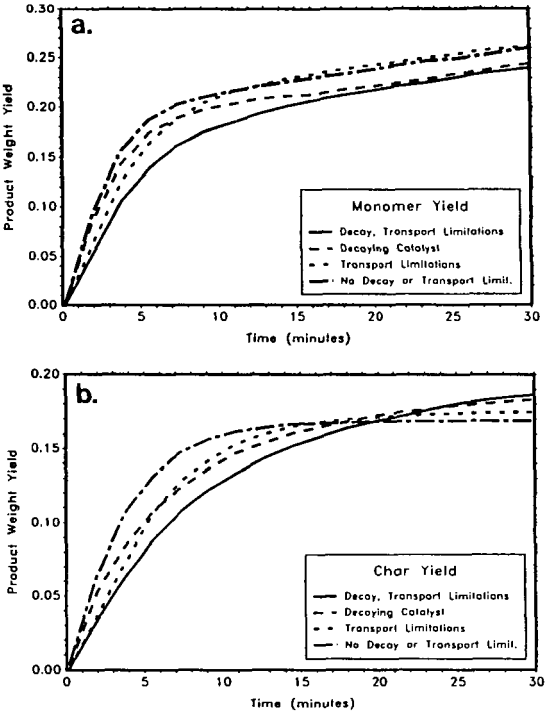

Figure 4: Effects of catalyst deactivation and transport limitations on lignin depolymerization (case 1). (a) monomer yield (b) char yield.

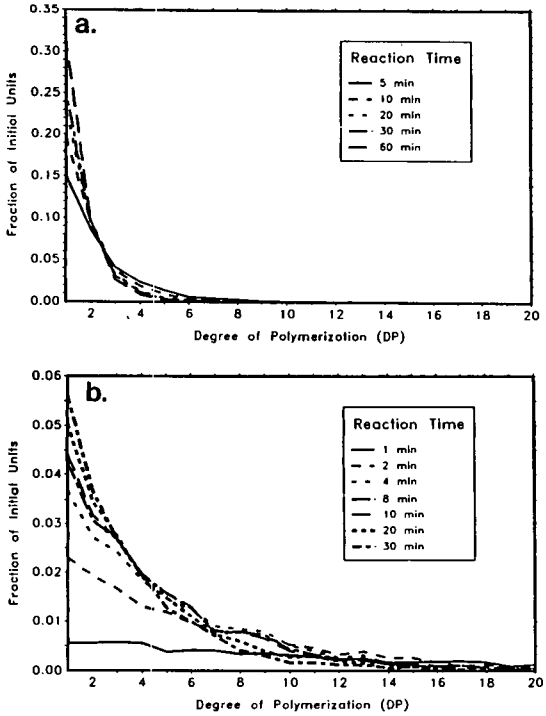

Figure 5: Temporal variation of the molecular weight distribution of a reacting lignin polymer. (a) catalytic (b) thermal

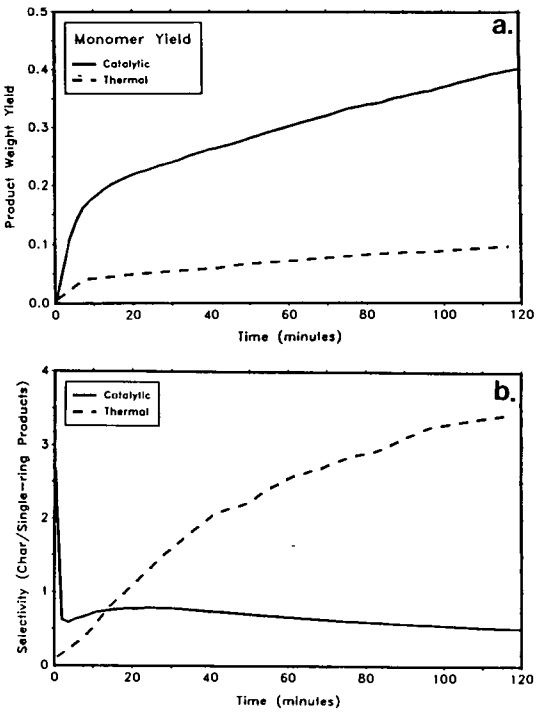

Figure 6: Comparison of thermal and catalytic liquefaction strategies. (a) monomer yield (b) selectivity (char/monomer)

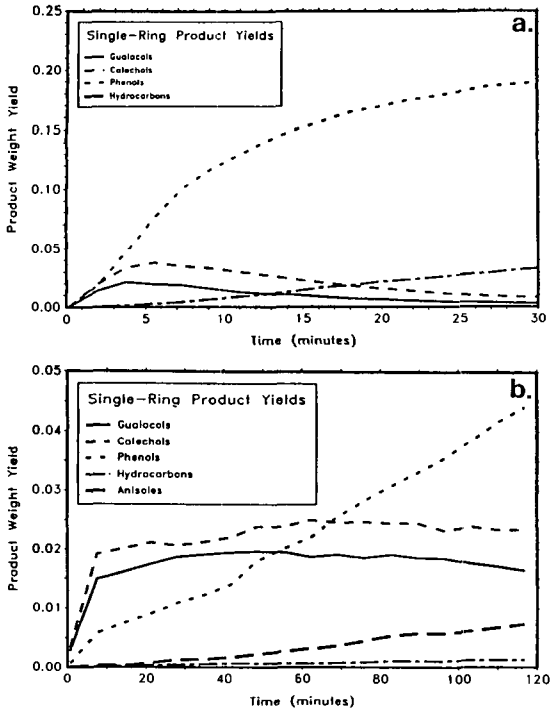

Figure 7: Comparison of single-ring product classes produced by thermal and catalytic liquefaction strategies. (a) catalytic (b) thermal

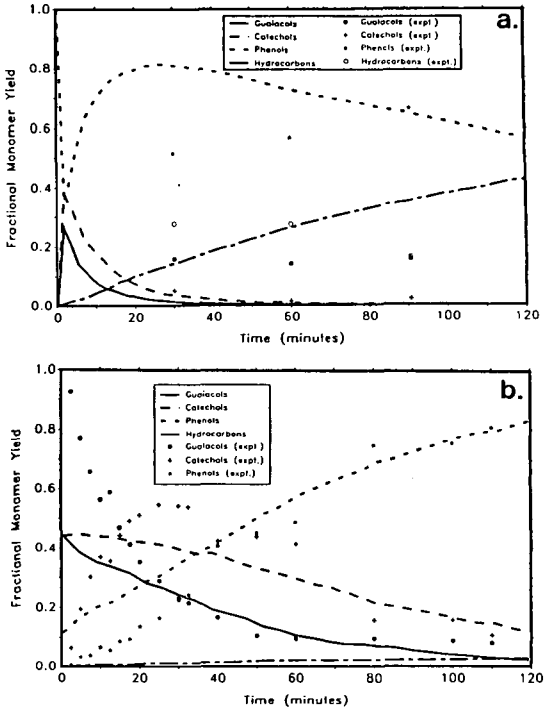

Figure 8: Comparison between simulation and experimental results. (a) catalytic (b) thermal